order Europa, Ganymede, and Callisto, $\sigma/\pi R^2$ at $\lambda = 0.13$ m is about 2.6, 1.5, and 0.6, whereas the cratering rates predicted by Shoemaker and Wolfe (*10*), when normalized to 2.6 for Europa, are 2.6, 1.3, and 0.7, respectively.

As used here, the descriptive term "buried craters" is meant to apply primarily to the electromagnetic model and only secondarily to the physical model. For example, in Fig. 1D, mechanical and thermal events during crater formation might compress or line the walls and produce a TIR source without the need for a later resurfacing flood. Craterlike geometry might also result from processes other than impacts; for example, differential freezing could create a source where the n_3 material of Fig. 1D fills the hemispheroidal n_2 void (*5*). This and the examples in Fig. 1, B, C, and D, all represent the electromagnetic model of buried craters. The most likely physical model is proposed here to be Fig. 1C.

Cratering and resurfacing have also occurred on rocky planets and Earth's moon. There are two reasons why the icy moons could display strong echoes from buried craters while the rocky bodies would not. The required TIR condition is plausible on icy moons but there is no comparable expectation for $n > 1$ interfaces on rocky bodies. Moreover, the loss coefficient for cold ice is much less than for the common minerals of the rocky surfaces, so that longer subsurface propagation paths are possible on the icy bodies.

There are three key requirements for further refinements in our understanding of the scattering process and its meaning in terms of the surface and subsurface characteristics of the three moons discussed here, and perhaps of dozens of other icy bodies in the outer solar system. First, the complete polarization properties of the echoes should be investigated by measuring either signal amplitudes at four polarizations or phase plus amplitude at two polarizations. Second, radar investigations using separated transmitters and receivers are needed to study scattering in other than the backward direction, and to determine how best to conduct radar mapping experiments. This could be done with powerful transmissions from Earth and reception at spacecraft near the targets (*11*). And finally, for all of the characteristics of the scattered radar signals there is a need for improved coverage and resolution so that detailed comparisons can be made with other sources of two-dimensional information, such as optical imaging.

REFERENCES AND NOTES

1. R. M. Goldstein and G. A. Morris, *Science* **188**, 1211 (1975); D. B. Campbell, J. F. Chandler, S. J. Ostro, G. H. Pettengill, I. I. Shapiro, *Icarus* **34**, 254 (1978); S. J. Ostro, D. B. Campbell, G. H. Pettengill, I. I. Shapiro, *ibid.* **44**, 431 (1980). Radar echoes from the icy moons are up to 2.6 times as strong as from perfectly reflecting metal spheres of the same size. Echoes from rocky planets and Earth's moon are roughly one-tenth the metal-sphere value. The polarization of waves reflected from rocky bodies is similar to that observed from large homogeneous spheres: incident waves polarized in the right-handed circular sense have echoes that are almost entirely polarized in the left-hand circular sense. Most of the energy in the echoes from the icy moons, however, is contained in the unexpected (right-handed in this case) circularly polarized component. Linearly polarized waves are also anomalously depolarized by the icy moons. For a homogeneous sphere, backscattered surface reflections come only from the center of the disk since off-normal incident rays are scattered in other directions. Although rocky-planet echoes are mainly from this central zone, the icy-moon echoes are strong from nearly all areas of the disk, so that, by comparison, the limbs appear to be unusually bright when observed by radar.
2. S. J. Ostro and G. H. Pettengill, *Icarus* **34**, 268 (1978).
3. R. M. Goldstein and R. R. Green, *Science* **207**, 179 (1980).
4. T. Hagfors, T. Gold, H. M. Ierkic, *Nature (London)* **315**, 637 (1985).
5. V. R. Eshleman, *ibid.* **319**, 755 (1986).
6. Radar cross section σ of a target is defined in such a way that $\sigma/\pi R^2 = 1$ for backscattering from a perfectly reflecting sphere of radius R large compared with the radar wavelength. For $N = 1$, $\sigma_1/\pi r_0^2 = (n - 1)^2/(n + 1)^2$. For $N \geqslant 2$, the glints have characteristic area $H\Delta r$ and radial width $\Delta r = (\lambda r_0 n_B/2n_c N)^{1/2}$. In the expression for σ_N, the magnitude of each ρ is unity for $n > n_c$, the condition for total internal reflection. The angle of incidence, measured between the ray direction and the normal to the crater wall at a reflection point, is nominally $(\pi/2)(1 - 1/N)$ so that $n_B = \tan(\pi/2N)$, $n_c = \sec(\pi/2N)$, and $n_c^2 = n_B^2 + 1$.
7. S. J. Ostro, in *Satellites of Jupiter*, D. Morrison, Ed. (Univ. of Arizona Press, Tucson, 1982), pp. 213–236.
8. For larger n, $x \rightarrow -1$ for all N. For smaller n and large N, x remains near zero until n is very close to zero, where it suddenly changes to $x = 1$ for even N and $x = -1$ for odd N at $n = 0$.
9. R. S. Saunders, T. J. Parkes, J. B. Stephens, E. G. Lane, F. P. Fanale, *Lunar Planet. Sci. Conf. Abstracts* **16**, 730 (1985).
10. E. M. Shoemaker and R. F. Wolfe, in *Satellites of Jupiter*, D. Morrison, Ed. (Univ. of Arizona Press, Tucson, 1982), pp. 277–339.
11. V. R. Eshleman *et al*, *Science* **223**, 772 (1984).

12. I thank G. L. Tyler, S. J. Ostro, R. A. Simpson, and T. Hagfors for helpful comments and discussion. Tyler had suggested an association of the radar observations with the glory even before the buried-crater model was devised. This work was supported by NASA.

12 May 1986; accepted 25 August 1986

Refractory Minerals in Interplanetary Dust

ROY CHRISTOFFERSEN* AND PETER R. BUSECK

A newly studied interplanetary dust particle contains a unique set of minerals that closely resembles assemblages in the refractory, calcium- and aluminum-rich inclusions in carbonaceous chondrite meteorites. The set of minerals includes diopside, magnesium-aluminum spinel, anorthite, perovskite, and fassaite. Only fassaite has previously been identified in interplanetary dust particles. Diopside and spinel occur in complex symplectic intergrowths that may have formed by a reaction between condensed melilite and the solar nebula gas. The particle represents a new link between interplanetary dust particles and carbonaceous chondrites; however, the compositions of its two most abundant refractory phases, diopside and spinel, differ in detail from corresponding minerals in calcium- and aluminum-rich inclusions.

INTERPLANETARY DUST PARTICLES (IDP's) and carbonaceous chondrite meteorites are two types of extraterrestrial materials known to contain unprocessed components of the early solar system. IDP's of the chondritic subgroup chemically resemble carbonaceous chondrites (*1*) and contain some of the same principal minerals (*2, 3*). However, they exhibit enough textural and detailed mineralogical differences from carbonaceous chondrites to leave unanswered many questions regarding the relative formation histories of the two materials.

An unresolved aspect of the relation between IDP's and carbonaceous chondrites concerns the differences in their so-called refractory minerals, that is, the phases considered to be the highest temperature products of the solar nebula (*4*). Unusual enstatite crystals within some IDP's show evidence of being high-temperature nebular condensates (*5*). This finding raised the expectation that some IDP's might also contain samples of the more refractory, calcium- and aluminum-rich phases predicted to form in the solar nebula (*4*). Such refractory nebular materials occur in calcium- and aluminum-rich inclusions (CAI's) from certain carbonaceous chondrites, meteorites in which the mineralogy, chemistry, and isotopic composition of CAI's have been studied intensely (*6*). To our knowledge, however, the identification of fassaite in one IDP sample (*7*) has been the only instance where a phase characteristic of CAI's has been found in a chondritic IDP, and refractory phases have largely remained the "missing links" of IDP mineralogy.

We report transmission electron micro-

Departments of Geology and Chemistry, Arizona State University, Tempe, AZ 85287.

*Present address: Department of Geology, Indiana University, Bloomington, IN 47405.

Table 1. Compositions of high-temperature minerals in the Spray IDP. Oxide abundances (in percentages by weight) are based on thin-film, energy-dispersive, x-ray analyses (*19*) obtained with an analytical TEM (Phillips 400T). Highest and lowest values among the analyzed grains are shown, except when only one grain was analyzed. Standard relative errors based on counting statistics are approximately 5% for oxide abundances greater than 1.0%, and 10% for abundances less than 1.0%.

Mineral	Nominal chemical formula	No. of grains analyzed	Composition (% by weight)				
			CaO	Al_2O_3	TiO_2	FeO	Cr_2O_3
Diopside	$CaMgSi_2O_6$	15	19.0–26.6	0.7–3.8		0.1–2.7	4.6, 8.1*
Spinel	$MgAl_2O_4$	3		67.7–73.1		0.5–1.3	1.7–2.7
Anorthite	$CaAl_2Si_2O_8$	3	18.0–19.8†	34.8–35.9†			
Fassaite	Ca(Mg, Ti, Al)(Al, Si)$_2$O$_6$	1	22.56	19.89	5.5	0.8	0.4
Perovskite	$CaTiO_3$	1	41.2		58.8		
Enstatite	$MgSiO_3$	6	0.4–1.9	0.0–2.5		2.4–7.4	0.2–0.8
Olivine	(Fe, Mg)$_2$SiO$_4$	6				0.3–19.5‡	

*Detected in two grains. †Grains show no detectable sodium; Al_2O_3 and CaO abundance ranges correspond to pure anorthite within analytical error. ‡Range corresponds to compositions from 99 to 77 mole percent of Mg_2SiO_4.

scope (TEM) observations of an IDP called "Spray" (*8*), which is the first IDP reported to contain several of the minerals that are typical of CAI's. The unique mineralogy of this particle presents possible new connections between IDP's and carbonaceous chondrites. Ion-probe analyses of fragments of Spray show that it contains highly deuterium-enriched material, indicating that it has a primitive hydrogen isotopic composition similar to that of components in certain carbonaceous chondrites (*9*). Infrared (IR) spectroscopic measurements have also shown that Spray is within the so-called pyroxene optical subgroup of IDP's, a class of micrometeorites whose IR properties are similar to those of cometary dust (*10*).

The original Spray particle (*10*) was a large (approximately 50 μm in diameter) chondritic-porous aggregate (*1*) that broke into several fragments upon impact with its collector plate. The largest of its pieces, Spray-1 and -2, were used for ion probe and IR spectroscopic analyses (*9, 10*). Another 10-μm-diameter fragment, Spray-8, was crushed and mounted on a carbon-film substrate for the present TEM study. (Subsequent descriptions refer to this fragment as it appears in partially disaggregated and dispersed form on its carbon-film TEM mount.)

Spray is texturally typical of chondritic IDP material. It is composed of crystalline grains, 0.1 to 0.5 μm in diameter, together with clumps of dense matrix material that has a grain size between 100 and 500 Å. In addition to small crystalline grains, the matrix has an amorphous component that has the chemical and diffraction characteristics of amorphous carbon or hydrocarbon.

The CAI-type minerals identified in Spray include diopside, spinel, anorthite, fassaite, and perovskite (Table 1). Diopside and spinel are the most abundant phases in the particle and occur as discrete anhedral crystals, or, more commonly, they are intergrown and form polycrystalline grains. In some cases these aggregates simply consist of a pair of diopside and spinel crystals attached along a straight grain boundary; elsewhere they are more complex and contain several diopside and spinel grains, individually 500 Å to 0.1 μm in diameter, intergrown with a complex symplectic structure. Dark-field imaging of two diopside grains revealed the presence of faint solar-flare ion tracks, confirming that Spray is extraterrestrial and that it has experienced no more than moderate heating upon entry into the atmosphere (*3, 11*). Anorthite, fassaite, and perovskite occur in small amounts as discrete, single crystals with irregular, anhedral morphologies. The fassaite displays multiple (100) twins; the anorthite exhibits a slight, mottled contrast but is otherwise featureless, as is the perovskite.

Spray also contains abundant, mostly anhedral, olivine and enstatite grains (Table 1). A few of the larger enstatite crystals are platy and roughly rectangular in outline. Electron diffraction patterns and lattice-fringe images of these platy grains show them to be untwinned clinoenstatites containing (100) stacking faults. The structure of the grains is similar to the IDP enstatite "ribbons" suspected of being condensate grains by Bradley and co-workers (*5*). However, compared to the clinoenstatite described in (*5*), the Spray clinoenstatite has a higher degree of stacking disorder. The platy enstatites in our sample are possibly fragments of ribbons that were broken during sample preparation, or at some earlier stage in the particle's history. Additional lower temperature phases that are present in Spray include nickel-bearing pyrrhotite, which occurs as spherules and angular grains, and magnetite, which forms dense masses of grains less than 500 Å in diameter within the matrix material.

When compared to most CAI's, the total mass and average grain size of the refractory component of Spray are small. However, the two materials can be compared. Our observations show that the refractory portion of Spray consists mostly of clinopyroxene (diopside) and spinel, and apparently little or no melilite [Ca_2(Mg, Al, Si)$_3$O$_7$] or hibonite ($CaAl_{12}O_{19}$). Therefore, the Spray refractory assemblage differs from the considerable number of CAI's that have melilite or hibonite as the principal components. Examples include the type A, coarse-grained inclusions in the Allende meteorite, which are composed predominantly of melilite and little or no clinopyroxene (*6*), and many of the hibonite- and melilite-rich objects in the Murchison meteorite (*12*).

The abundance and the intimate textural association of spinel and clinopyroxene in Spray specifically suggest a connection to the subset of CAI's that consists predominantly of these two phases (*13–17*). To explore this possible correlation, we can compare the compositions of the clinopyroxene and spinel in Spray to counterparts that occur as major components in CAI's from various carbonaceous chondrites (Fig. 1). Since there is textural evidence that the spinel and clinopyroxene in Spray were associated in their formation, Fig. 1 incorporates data only for CAI's, or portions of CAI's, where spinel and clinopyroxene are intergrown or in contact. [For example, data from certain CAI rims, in which spinel and clinopyroxene apparently formed separately (*18*), are excluded.]

There is only partial concordance between the spinel and clinopyroxene compositions in Spray and those in CAI's (Fig. 1). Although the Spray spinel is similar in its low FeO content to that in both coarse-grained and certain fine-grained CAI's, the spinel is also measurably higher in Cr_2O_3. Spray spinel has considerably less FeO than the hercynitic spinels characteristic of Allende fine-grained CAI's. The clinopyroxene in Spray has no detectable TiO_2 and differs in this respect from the fassaitic pyroxenes in Allende type B inclusions and in fine-grained CAI's from other meteorites. Although there is some overlap between the Spray clinopyroxene composition and those in fine-grained CAI's from Allende and Efremovka meteorites, only the Efremovka CAI's also have spinel compositions that approach those in Spray.

The differences in mineralogy and mineral chemistry between the refractory assemblage in Spray and the CAI's considered above are not surprising, considering the variations that occur among the CAI's themselves. The variability among CAI's is widely considered to reflect formation by diverse nebular processes, including gas-to-solid (or liquid) condensation reactions, fractional evaporation, and melting (*13–17*). We cannot exclude any of these processes as sources of the Spray refractory components, yet several aspects of the Spray refractory assemblage appear to be most consistent with formation by predicted condensation reactions.

In particular, a mechanism for formation of the diopside-spinel association in Spray is suggested by the condensation reaction:

$$\text{melilite} + \text{vapor} \rightarrow \text{spinel} + \text{diopside}$$

which occurs at 1450 K (pressure is 10^{-3} atm) in the sequence calculated by Grossman (*4*). The reaction describes the breakdown of condensed melilite in the nebular gas to form a mixture of diopside and spinel. The result should be a mineral assemblage that, similar to the assemblage in Spray, lacks melilite and contains aggregates of intimately intergrown, relatively pure, spinel and diopside. Grossman's calculations also predict that perovskite, another Spray constituent, should be in equilibrium with spinel and diopside in the temperature range 1450 to 1393 K. Anorthite forms at a lower temperature (1362 K) when spinel is consumed by excess diopside (*4*). The small amount of anorthite in Spray, and the varying amounts of aluminum in its diopside (Fig. 1a), may be the result of partial progress of this reaction.

The condensation sequence as described above is subject to the uncertain role of fassaite as a condensate in place of one or more of the above phases (*6*), and thus the preceding arguments are tentative. Circumstantial support for a condensation origin of the refractory part of Spray is provided by the several enstatite grains in the particle that closely resemble other IDP enstatites thought to be direct condensates (*5*).

Apart from the question of precisely which processes formed its refractory components, Spray clearly adds diversity to IDP mineralogy. Its discovery starts to close gaps between IDP's and some of the most primitive varieties of meteorites. Continued characterization of IDP's, particularly in an attempt to identify refractory phases, may close this gap still further and provide additional insights into early solar system processes.

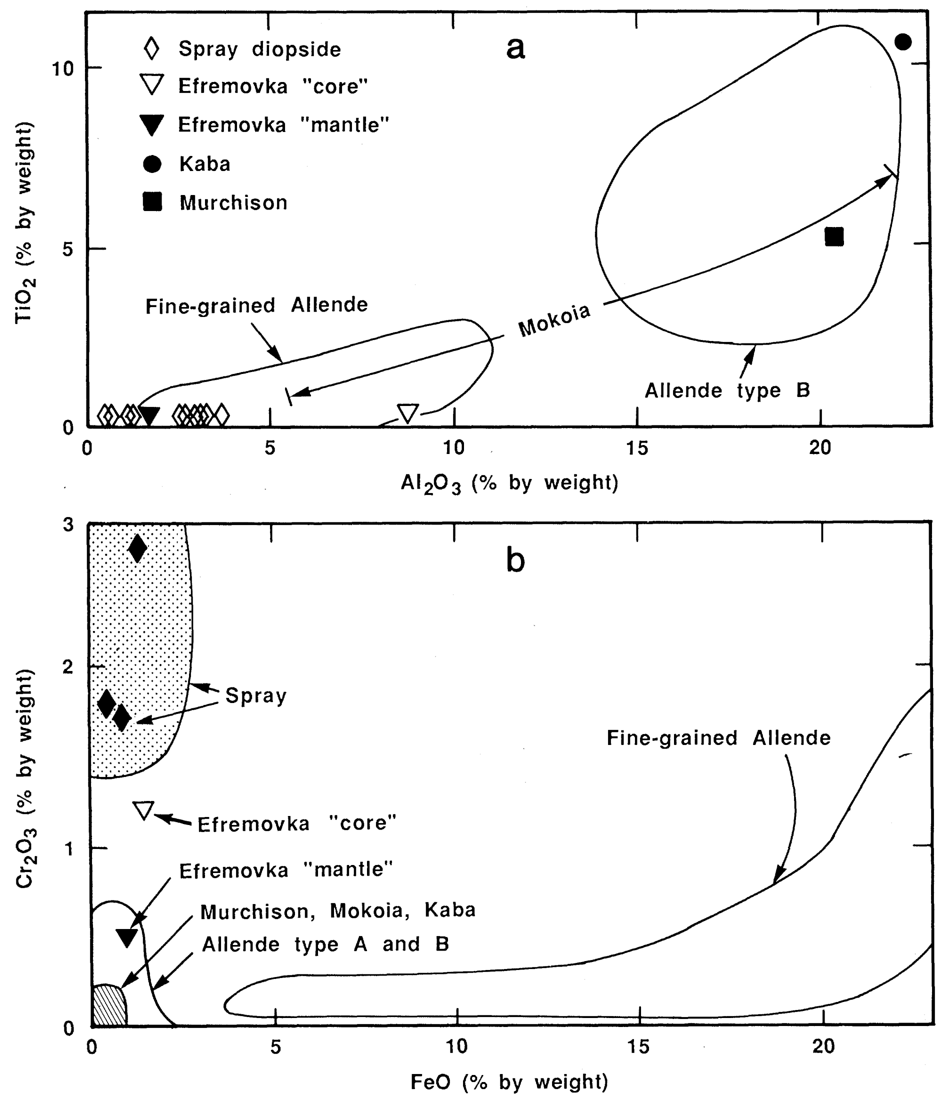

Fig. 1. Clinopyroxene (a) and spinel (b) compositions in Spray (diamonds) compared to those in CAI's from various carbonaceous chondrite meteorites. Mineral compositions in meteorites were obtained from the following references: Efremovka (*14*), Kaba (*17*), Murchison (*12*), Mokoia (*16, 20*), fine-grained Allende (*13*), and Allende types A and B (*15*). Table 1 gives analytical TEM methods and analytical error estimates. The relatively small number of spinel analyses from Spray reflects the comparative scarcity of separate spinel grains in the sample. The stippled region in (b) gives estimated range of spinel compositions based on analyses of the abundant spinel-clinopyroxene aggregates.

REFERENCES AND NOTES

1. D. E. Brownlee, E. Olsziewski, M. Wheelock, *Lunar Planet. Sci.* **13**, 71 (1982).
2. P. Fraundorf, *Geochim. Cosmochim. Acta* **45**, 915 (1981).
3. R. Christoffersen and P. R. Buseck, *Earth Planet. Sci. Lett.* **78**, 53 (1986).
4. L. Grossman, *Geochim. Cosmochim. Acta* **36**, 597 (1972).
5. J. P. Bradley, D. E. Brownlee, D. R. Veblen, *Nature (London)* **301**, 473 (1983).
6. L. Grossman, *Annu. Rev. Earth Planet. Sci.* **8**, 559 (1980).
7. K. Tomeoka and P. R. Buseck, *Nature (London)* **314**, 338 (1985).
8. Spray was collected in the stratosphere by a NASA U-2 aircraft (Spray designation, u23-M4-4).
9. K. D. McKeegan, R. M. Walker, E. Zinner, *Geochim. Cosmochim. Acta* **49**, 1971 (1985).
10. S. A. Sandford and R. M. Walker, *Astrophys. J.* **291**, 838 (1985).
11. J. P. Bradley, D. E. Brownlee, P. Fraundorf, *Science* **226**, 1432 (1984).
12. G. J. MacPherson, M. Bar-Matthews, T. Tanaka, E. Olsen, L. Grossman, *Geochim. Cosmochim. Acta* **47**, 823 (1983).
13. A. S. Kornacki and J. A. Wood, *ibid.* **49**, 1219 (1985).
14. D. A. Wark, A. S. Kornacki, W. V. Boynton, A. A. Ulyanov, *Lunar Planet. Sci.* **17**, 921 (1986).
15. L. Grossman, *Geochim. Cosmochim. Acta* **39**, 433 (1975).
16. R. E. Cohen, A. S. Kornacki, J. A. Wood, *ibid.* **47**, 1739 (1983).
17. B. Fegley and J. E. Post, *Earth Planet. Sci. Lett.* **75**, 297 (1985).
18. D. A. Wark and J. F. Lovering, *Proc. Lunar Sci. Conf.* **8**, 95 (1977).
19. G. Cliff and G. W. Lorimer, *J. Microsc. (Oxford)* **103**, 203 (1975).
20. K. Tomeoka, personal communication.

21. We thank R. M. Walker for providing the Spray IDP sample. Discussions with R. A. Walker, S. A. Sandford, and K. Tomeoka are gratefully acknowledged. Electron microscopy was performed at the electron microscopy facility in the Center for Solid State Science, Arizona State University. Supported by NASA grant NAG 9-59.

5 May 1986; accepted 5 August 1986